Influence of Proline Position upon the Ion Channel Activity of Alamethicin

Christine Kaduk,* Hervé Duclohier,# Margitta Dathe,* Holger Wenschuh,* Michael Beyermann,* Gérard Molle,# and Michael Bienert*

*Forschungsinstitut für Molekulare Pharmakologie, 10315 Berlin, Germany, and #URA 500 CNRS, Université de Rouen, 76821 Mont-Saint-Aignan, France

ABSTRACT Alamethicin, a 20-residue peptaibol, induces voltage-dependent ion channels in lipid bilayers according to the barrel-stave model. To study relationships between the proline-14-induced kink region and the channel-forming behavior of the peptide, a set of alamethicin analogs with proline incorporated at positions 11, 12, 13, 14, 15, 16, and 17, respectively, as well as an analog with alanine instead of proline at position 14 were synthesized. Macroscopic conductance experiments show that the voltage dependence of the peptides is conserved although slightly influenced, but the apparent mean number of monomers forming the channels is significantly reduced when proline is not located at position 14. This is confirmed in single-channel experiments. The analogs with proline next to position 14 (i.e., 13, 15, 16) show stable conductance levels, but of reduced number, which follows the order Alam-P14 > Alam-P15 > Alam-P16 > Alam-P13. This reduction in the number of levels is connected with changes in the lifetime of the channels. Analogs with proline at position 11, 12, or 17 produce erratic, extremely short-lived current events that could not be resolved. The changes in functional properties are related to structural properties as probed by circular dichroism. The results indicate that proline at position 14 results in optimal channel activity, whereas channels formed by the analogs bearing proline at different positions are considerably less stable.

INTRODUCTION

Alamethicin is a 20-amino acid-containing peptaibol, originally isolated from the fungi *Trichoderma viride* (Meyer and Reusser, 1967). The peptaibols are structurally related, amphipathic peptides containing a high percentage of the hydrophobic α-aminoisobutyric acid (Aib) residues and bearing an acetyl residue at the N-terminus as well as an α-amino alcohol at the C-terminus. A characteristic property of alamethicin is the ability to form well-resolved, voltage-dependent, multistate ion channels (Gordon and Haydon, 1972, 1975; Boheim, 1974). Different channel models have been described for understanding the mechanism of channel formation and transition among different conductance states (see reviews by Woolley and Wallace, 1992; Sansom, 1991, 1993; Cafiso, 1994). The widely accepted model is the so-called barrel-stave model (Baumann and Mueller, 1974; Boheim, 1974). According to this model the alamethicin channel is built by a bundle of helical monomers forming a water-filled transmembrane pore through which ions can cross lipid membranes. An association of 3 to 12 helical monomers is suggested to determine the different conductance levels.

Previous NMR studies led to the conclusion that the peptide forms a relatively rigid, largely helical rod with a less well-defined C-terminus (Esposito et al., 1987; Chandrasekhar et al., 1988; Kelsh et al., 1992). More recent investigations confirm a high flexibility in the central portion of the peptide in solution as well as in a micellar environment (North et al., 1994; Franklin et al., 1994; Yee et al., 1995). This break from the strong helix tendency in the N-terminus may result from Pro 14 and the loss of helix-stabilizing hydrogen bonding in this portion of the structure.

Because the exact conformation of alamethicin in the channel-forming states cannot be determined at present, the mechanism underlying the transition among different conductance states as well as the opening-closing mechanism are still a matter of debate. According to Fox and Richards (1982), the channel opening-closing mechanism implies some reorientation of the C-terminal part of the peptide molecules in the presence of the electric field. This conformational change was suggested to occur around the proline residue 14, which is supposed to play a key role in the function of alamethicin channels. The crucial role of the proline residue is supported by a relatively high frequency of the residue in a number of peptaibols and, putatively, α-helical transmembrane segments of many integral membrane proteins acting as receptor subunits, channels, or transporters (Woolfson et al., 1991; Vogel et al., 1993; Vanhoof et al., 1995). Furthermore, the observation that non-Aib-containing synthetic analogs of alamethicin with the substitution of proline (Pro) in position 14 by alanine (Ala) retain their channel-forming ability and voltage sensivity, but exhibit considerably reduced lifetimes (Duclohier et al., 1992), underlines the role of proline in channel opening-closing kinetics, although it might not be essential for the gating process per se.

Although a number of attempts have been made to rationalize the role of proline 14 in the channel-forming properties of alamethicin (Duclohier et al., 1992; Brachais et al., 1995b), systematic structure-activity relationships could not

Received for publication 29 October 1996 and in final form 6 February 1997.

Address reprint requests to Dr. Margitta Dathe, Forschungsinstitut für Molekulare Pharmakologie, Alfred-Kowalke-Strasse 4, D-10315 Berlin, Germany. Tel.: 49-30-51551305; Fax: 49-40-51551206; E-mail: dathe@fmp-berlin.de.

0006-3495/97/05/2151/09 $2.00

be examined, because of the lack of reliable methods to synthesize analogs. Recently, Fmoc-amino acid fluorides have been shown to be well suited for the solid-phase synthesis of peptides incorporating sterically hindered residues such as α-aminoisobutyric acid (Wenschuh et al., 1995). To analyze the influence of proline position upon ion channel formation of alamethicin systematically, this powerful tool was used to synthesize a set of six alamethicin analogs with proline displaced either upward or downward to position 14 (for sequences see Table 1). Furthermore, an alamethicin analog where Pro^{14} was substituted by Ala was synthesized. The functional properties of these analogs were compared both in macroscopic and in single-channel conductance experiments after incorporation of the peptides in planar lipid bilayers and related to structural properties, as determined by circular dichroism (CD).

MATERIALS AND METHODS

Synthesis of peptides

The alamethicin peptides were synthesized by the solid-phase technique, using Fmoc-protected amino acid fluorides, which were prepared via (diethylamino)sulfur trifluoride (Kaduk et al., 1995). The peptide assembly was carried out on a MPS synthesizer ACT 348 (Advanced ChemTech, Louisville, KY) as described previously (Wenschuh et al., 1995). After completion of the synthesis and acetylation of the N-terminus, the peptides were released from the resin by treatment with 2% triisopropylsilane and 5% water in 50% trifluoroacetic acid (TFA)/dichloromethane (DCM) for 45 min to give the N-acetylated free peptide. The purified peptides were characterized by reversed-phase high-performance liquid chromatography and electrospray ionization mass spectrometry (ESI-MS).

Circular dichroism experiments

Vesicle preparation

Small unilamellar vesicles (SUVs) for CD measurements were prepared by suspending and vortexing the dried lipid in buffer (10 mM Tris, 154 mM NaF, 0.1 mM EDTA, pH 7.4) to give final lipid concentrations between 20 and 40 mM. The suspensions were sonicated (under nitrogen in an ice bath) for 25 min using a titanium tip ultrasonicator. Titanium debris was removed by centrifugation. Dynamic light scattering experiments (N4 Plus; Coulter Corporation, Miami, FL) confirmed the existence of a main population of vesicles (more than 95% mass content) with a mean diameter of 46 $\pm$ 1 nm (polydispersity index 0.3).

CD measurements

Stock peptide solutions were prepared by dissolving the samples in methanol. Aliquots of the peptide solution, buffer, and SUV suspension were mixed to reach the desired peptide concentration and solvent composition. The methanol content was less than 5%. CD measurements were carried out on a J 720 spectrometer (Jasco, Japan) between 250 and 200 nm at room temperature. Six CD scans were usually accumulated for each sample, and at least two independent preparations for each type of sample were measured, smoothed, and averaged. Circular dichroism and differential scattering of the SUVs were eliminated by subtracting the spectra of the corresponding peptide-free suspensions. The helicity was determined from the mean residue ellipticity $[\Theta]$ at 222 nm according to the relation $[\Theta]_{222} = -30300\,[\alpha] - 2340$ ($[\alpha]$ being the amount of helix) (Chen et al., 1972). The error was 5% helicity.

Macroscopic and single-channel conductance experiments

Macroscopic and single-channel conductance experiments were performed with planar lipid bilayers formed over 175-μm- and 125-μm-diameter holes, respectively, in a 25-μm-thick Teflon film (PTFE; Goodfellow, Cambridge, England). The Teflon film was sandwiched between two glass half-cells and pretreated with hexane/hexadecane (40:1, v/v) (Fluka, spectroscopic grade). For both macroscopic and single-channel conductance experiments, the lipid mixture used was 1-palmitoyl-2-oleoyl-phosphatidylcholine (POPC)/dioleoylphosphatidylethanolamine (DOPE) (from Avanti Polar Lipids, Alabaster, AL) (7:3, w/w). The electrolyte solution was 1 M KCl. The lipid dissolved in *n*-hexane was spread on the surface of electrolyte solution in both compartments. Bilayer formation was achieved by lowering and raising the level in one or both reservoirs (Montal and Mueller, 1972) and was monitored by the capacity response. Before adding the peptide from a methanolic stock solution to the *cis* (or positive) side (final methanol concentration was less than 5%), the bare membrane was checked under an applied potential for stability and absence of channel-like events.

For the macroscopic conductance experiments, currents were measured using a Keithly amplifier (model 427; Cleveland, OH). The current-voltage curves were generated in response to triangular voltage ramps (up to $\pm$ 200 mV, 40 s/cycle) and recorded on a chart recorder. Three to five such ramps were recorded for each compound and concentration. The characteristic parameters determined from each scan differed by no more than 5%.

Single-channel events were recorded using a BLM-120 amplifier (Bio-Logic, Claix, France) with a CV-5-1G headstage (gain: 1 mV/pA). The current fluctuations were filtered at 1 kHz for Alam-P13, Alam-P14, Alam-P15, Alam-P16, and Alam-A14, and the filter was set at 10 kHz for Alam-P11, Alam-P12, and Alam-P17. Recordings were stored on a digital tape recorder (DTR 1200; Bio-Logic) and analyzed with Satori v. 3.01 software from Intracel (Cambridge, England).

RESULTS

Synthesis

Alamethicin and the seven analogs (for sequences see Table 1), synthesized via Fmoc-amino acid fluoride strategy, were obtained with at least 97% purity as checked by

TABLE 1 Amino acid sequences of alamethicin F 30 (Alam-P14) and the seven examined alamethicin analogs

	1	14	20
Alam-P11:	Ac-Aib-Pro-Aib-Ala-Aib-Ala-Gln-Aib-Val-Aib-**Pro**-Gly-Leu-Aib-Val-Aib-Aib-Glu-Gln-Pheol		
Alam-P12:	Ac-Aib-Pro-Aib-Ala-Aib-Ala-Gln-Aib-Val-Aib-Gly-**Pro**-Leu-Aib-Val-Aib-Aib-Glu-Gln-Pheol		
Alam-P13:	Ac-Aib-Pro-Aib-Ala-Aib-Ala-Gln-Aib-Val-Aib-Gly-Leu-**Pro**-Aib-Val-Aib-Aib-Glu-Gln-Pheol		
Alam-P14:	Ac-Aib-Pro-Aib-Ala-Aib-Ala-Gln-Aib-Val-Aib-Gly-Leu-Aib-**Pro**-Val-Aib-Aib-Glu-Gln-Pheol		
Alam-P15:	Ac-Aib-Pro-Aib-Ala-Aib-Ala-Gln-Aib-Val-Aib-Gly-Leu-Aib-Val-**Pro**-Aib-Aib-Glu-Gln-Pheol		
Alam-P16:	Ac-Aib-Pro-Aib-Ala-Aib-Ala-Gln-Aib-Val-Aib-Gly-Leu-Aib-Val-Aib-**Pro**-Aib-Glu-Gln-Pheol		
Alam-P17:	Ac-Aib-Pro-Aib-Ala-Aib-Ala-Gln-Aib-Val-Aib-Gly-Leu-Aib-Val-Aib-Aib-**Pro**-Glu-Gln-Pheol		
Alam-A14:	Ac-Aib-Pro-Aib-Ala-Aib-Ala-Gln-Aib-Val-Aib-Gly-Leu-Aib-**Ala**-Val-Aib-Aib-Glu-Gln-Pheol		

reversed-phase high-performance liquid chromatography. ESI-MS provided the correct molecular masses for alamethicin and the proline analogs ($[M+Na]^+_{found}$: 1987 Da, $[M+Na]^+_{calculated}$: 1986 Da), showing that the peptides have identical amino acid composition. The equivalence of the calculated and determined masses for the Alam-A14 analog ($[M+Na]^+_{found}$: 1962 Da, $[M+Na]^+_{calculated}$: 1962.3 Da) confirms the identity of the peptide.

Secondary structures

The conformational properties of the examined peptides are reflected by the CD spectra in Fig. 1 and the calculated helicity (Table 2). All peptides show little regular structure in aqueous solution. In the presence of liposomes composed of phosphatidylcholine, alamethicin exhibits a helicity of about 45%. The fact that the helical content does not change with increasing lipid concentration above 5.2 mM (Table 2) reveals that the peptide is completely bound. Replacement of Pro^{14} by Ala doubles the helical content (Fig. 1, Table 2). The helical content of Alam-P16 is almost identical to that of the parent peptide, but Alam-P13 and Alam-P15 show significantly lower helicity. The amount of α-helix of Alam-P11, Alam-P12, and Alam-P17 continuously increases with enhancing lipid concentration, reflecting a reduced binding affinity.

Functional properties

All analogs induce voltage-dependent current changes, as shown by macroscopic current-voltage curves (*I-V* curves)

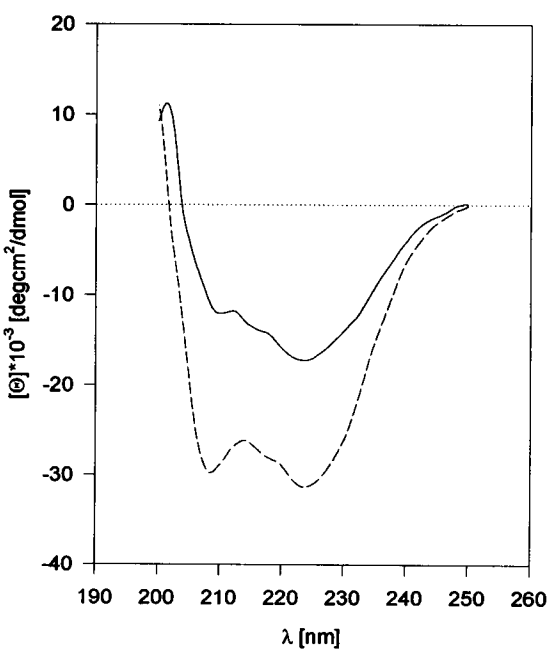

FIGURE 1 Circular dichroism spectra of 2.5×10^{-5} M Alam-P14 (——) and of 2.5×10^{-5} M Alam-A14 (– – –) bound to POPC vesicles (5.2×10^{-3} M) at room temperature.

in Figs. 2 and 3. Comparison of the conductivity induced by Alam-P14 and Alam-A14 reveals that the native peptide is much more effective in reducing the barrier function of the bilayer than is the Alam-A14 analog (Fig. 2). Whereas the characteristic voltage V_c (defined here as the voltage required to reach a reference conductance of 25 nS) for Alam-P14 (peptide concentration 8×10^{-8} M) was 65 mV, V_c for Alam-A14 was found to be 136 mV under identical conditions. Furthermore, differences in the hysteresis of the two *I-V* curves already reveal significantly different kinetics in the conductance states of the two peptides. The reference conductance ($S = 25$ nS) at 100 mV was usually reached by using an Alam-P14 concentration as low as 4×10^{-8} M (data not shown). The different activity of alamethicin analogs with modified proline position is reflected by serious differences in the peptide concentration necessary to get *I-V* curves in the 100-mV voltage range (Fig. 3). Compared to Alam-P14, a 20-fold higher concentration for Alam-P15, Alam-P16, Alam-P17, and even a 100 times higher concentration for Alam-P12 and Alam-P13 had to be used. Comparing the *I-V* curves of Alam-P15 and Alam-P16 versus Alam-P13 (Fig. 3 *A*) and Alam-P17 versus Alam-P12 (Fig. 3 *B*), it is interesting to note that substitutions of the more central amino acid residues (12, 13) by proline are much more effective in reducing the activity than shifting proline into the C-terminal positions 15, 16, 17. Moreover, a significant hysteresis in the *I-V* curves was observed for Alam-P13, Alam-P15, Alam-P16 as compared to analogs with proline at position 12 or 17.

The characteristic parameters reflecting the influence of the individual peptides on the macroscopic electrical properties of the lipid bilayer are summarized in Table 3. The data were derived by analyzing the macroscopic *I-V* curves as described by Hall et al. (1984). Profound differences appeared when the concentration dependence of the peptides was studied. For this investigation the peptide concentration was doubled in several steps, and after we ensured that equilibrium was reached, the characteristic voltage V_c was read. The slope of the line representing V_c as a function of the logarithm of peptide concentration gives the parameter V_a, which is the characteristic voltage shift caused by an e-fold change in peptide concentration and thus reflecting the concentration dependence of activity. Compared to the native alamethicin, all analogs exhibit a reduced concentration dependence, as demonstrated in Table 3. Moreover, differences in the voltage dependence were observed. All analogs, except Alam-P17, present a slightly reduced voltage dependence, as shown by their higher V_e values (Table 3), which give the voltage increment producing an e-fold change in conductance at a given peptide concentration. The apparent number of monomers $\langle N \rangle$ forming the conducting aggregates can be simply determined by the relation $\langle N \rangle = V_a/V_e$. For alamethicin, an apparent number of 10 monomers building up the ion channels was calculated, whereas for the analogs $\langle N \rangle$ was found to be significantly reduced (Table 3).

Figs. 4, 5, and 6 exhibit typical single-channel current traces induced by the examined peptaibols in phosphatidyl-

TABLE 2 Helicity of alamethicin analogs in buffer and in the presence of SUVs composed of phosphatidylcholine

Peptide/ POPC-SUV	AlamP11	AlamP12	AlamP13	**AlamP14**	AlamP15	AlamP16	AlamP17	AlamA14
Buffer	8%	18%	7%	**7%**	6%	8%	5%	18%
2.6 mM	11%	43%	22%	**41%**	13%	40%	27%	63%
5.2 mM	24%	65%	25%	**46%**	22%	42%	28%	90%
10.4 mM	52%	85%	27%	**44%**	24%	42%	38%	93%

The peptide concentration was 2.5×10^{-5} M, the solvent 10 mM Tris, 154 mM NaF, 0.1 mM EDTA, pH 7.4, containing 5% (v/v) methanol.

choline/phosphatidylethanolamine bilayers. Both Pro substitution by Ala and the change in the position of the proline residue seriously impeded channel formation with the analogs. The values of detectable conductance levels observed with Alam-A14-exposed bilayers closely resemble the levels seen with the native peptide (Fig. 4, *A* and *B*; Table 4). However, the number of detectable levels decreases from seven (Alam-P14) to four (Table 4). Furthermore, the lifetimes of events were reduced by more than 10-fold, revealing a substantial reduction in channel stability (Table 5). Moreover, Alam-P13, Alam-P15, and Alam-P16 produce stable conductance states; however, their number is reduced compared to Alam-P14 (Fig. 5). Interestingly, the conductance levels induced by the different peptides are almost identical (Table 4). With respect to their number, the activity follows the order Alam-P14 > Alam-P15 > Alam-P16 > Alam-P13, which correlates with macroscopic conductance data (Table 3). This reduction in the number of levels is matched with a change in the lifetime of the channels (Table 5). Long-living open states were observed for Alam-P13 (118 ms) in the first detected level at about 150 pS and for Alam-P15 (56 and 88 ms) at levels one (140 pS) and three (1400 pS), respectively. Alam-P11, Alam-P12, and Alam-P17 produce erratic, extremely short-lived current events that could not be resolved (Fig. 6). This was already apparent from the narrow hysteresis of the macroscopic *I-V* curves, which revealed very fast kinetics of current fluctuations.

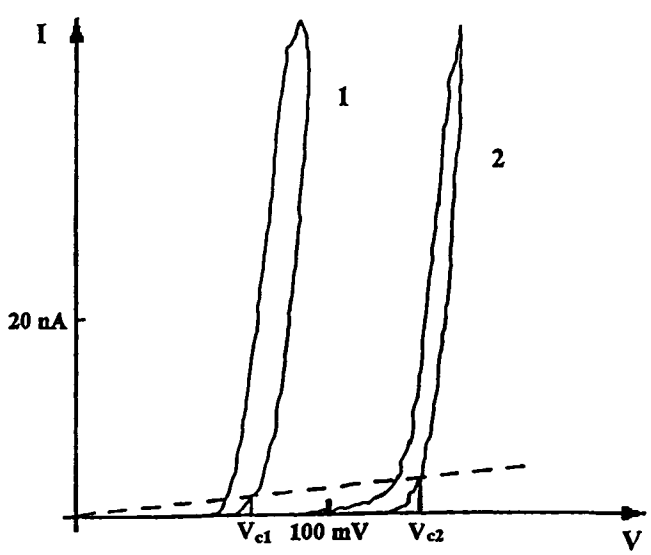

FIGURE 2 Macroscopic current-voltage curves at a POPC/DOPE bilayer for 8×10^{-8} M Alam-P14 (*curve 1*) and 8×10^{-8} M Alam-A14 (*curve 2*). The dashed line represents a reference conductance of 25 nS. V_{c1} = 65 mV, V_{c2} = 136 mV (see text). The panel shows a representative *I-V* curve out of three to five records that did not differ in the characteristic parameters by more than 5%.

DISCUSSION

According to the original barrel-stave model (Baumann and Mueller, 1974), the properties of alamethicin channels will depend on the number of monomers in the ion-conducting aggregates. An increase or reduction in the number of incorporated molecules will determine the change in the conduction level (Boheim, 1974). The number of associated monomers, their packing density in the channel arrangement, as well as the kinetics of monomer uptake and release are expected to depend on the orientation of the individual molecule and the conformational properties of the peptide in the membrane-bound state. This paper investigates the role of Pro^{14} in alamethicin for ion channel formation by comparing the activity of the native peptide with an analog containing an alanine at position 14 and peptides with proline shifted to the N- or C-terminus of the chain.

The results clearly show 1) The native peptide, Alam-P14, is the most effective channel-forming sequence, as confirmed by the low peptide concentration necessary to induce pore formation, and by the high number of detectable conductance levels and open states of the most probable levels ranging between 10 and 96 ms. 2) Pro^{14} substitution by Ala conserves the high voltage sensivity. However, higher concentrations are necessary to promote ion current, and a reduced number of conductance levels and significantly reduced lifetimes reflect the diminished channel-forming activity. 3) A proline shift next to position 14 (13, 15, 16) results in analogs that are also able to form ion channels, but at a reduced number of conductance levels, and changes in the probability of being open. 4) Analogs with proline at position 11, 12, or 17 induce voltage-dependent changes in ion permeability by very rapid bursts of activity, which are indicative of extremely unstable conductance states.

The discrete conductance levels ranging from 170 to 7200 pS and their number, the frequency of channel events, and the lifetimes observed in alamethicin (Alam-P14)-exposed bilayer correspond to earlier reports, particularly by Hanke and Boheim (1980). In agreement with a study of

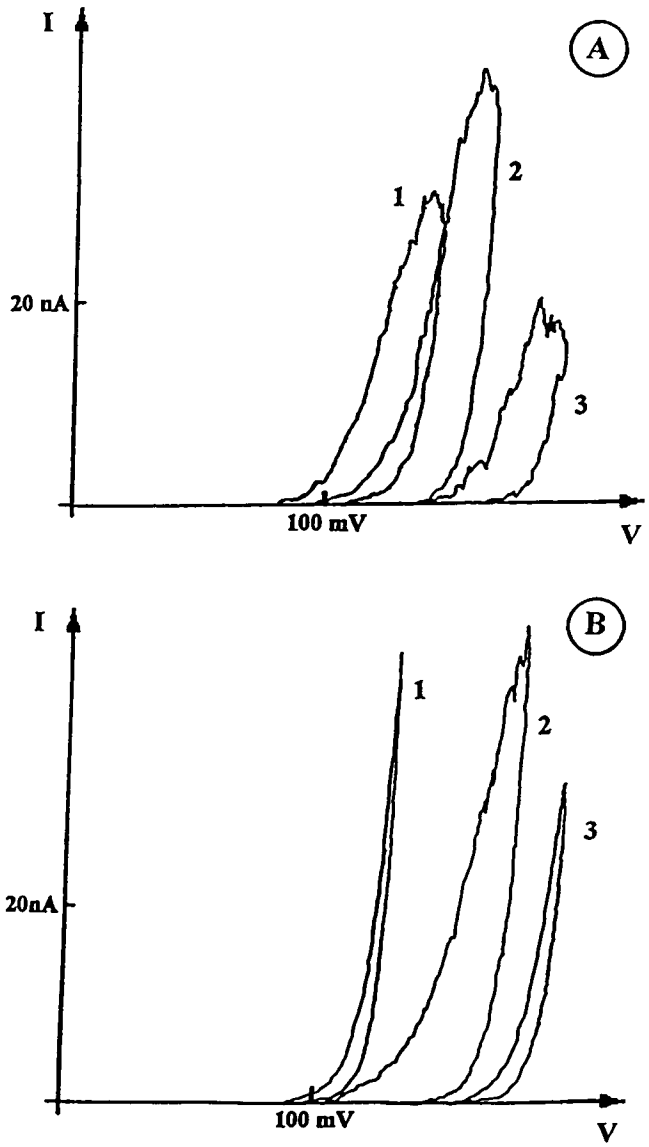

FIGURE 3 Macroscopic current-voltage curves at a POPC/DOPE bilayer, 1 M KCl both sides and room temperature (*A*) 5×10^{-7} M Alam-P15 (*curve 1*), 5×10^{-7} M Alam-P16 (*curve 2*), and 5×10^{-7} M Alam-P13 (*curve 3*). (*B*) 8×10^{-7} M Alam-P17 (*curve 1*), 1.5×10^{-7} M Alam-P11 (*curve 2*), and 8×10^{-7} M Alam-P12 (*curve 3*). *A* and *B* show a representative *I-V* curve out of three to five records that did not differ in the characteristic parameters by more than 5%.

TABLE 3 Macroscopic conductance parameters yielding the concentration dependence, the voltage dependence, and the apparent mean number of peptide molecules forming the channel

Peptide	Concentration dependence, V_a (mV)	Voltage dependence, V_c (mV)	Apparent mean no. of monomers, $\langle N \rangle$
Alam-P11	50	8	6
Alam-P12	45	7	6
Alam-P13	35	9	4
Alam-P14	**60**	**6**	**10**
Alam-P15	45	9	5
Alam-P16	41	8	5
Alam-P17	40	5	8
Alam-A14	38	6	6

The data are the mean of the results of three to five experiments, which differ by less than 5%.

Duclohier et al. (1992) comparing the activity of Pro^{14} and Ala^{14} alamethicin analogs containing Leu instead of Aib, our investigations with Alam-P14 and Alam-A14 confirm that proline substitution substantially reduces channel activity. The significant lower $\langle N \rangle$ derived for Alam-A14 from macroscopic conductance experiments correlates with the reduction of the number of detectable conductance levels. The observation leads to the conclusion that Alam-A14 is not able to form large stable associates. As observed with the corresponding Leu analogs (Duclohier et al., 1992), the stability of the detected states of Alam-A14 is also significantly reduced. The Ala^{14} analog induces much faster current fluctuations than the native peptide. This is surprising at first glance, because the replacement of Pro by Ala restores the helix conformation in the central part of the molecule, as observed by a substantial increase in peptide helicity in the presence of lipid vesicles composed of phosphatidylcholine. The stabilization of helical structure is in accordance with NMR studies of the Alam-A14 analog (Brachais et al., 1995a), in which all Aib were replaced by Leu. However, it seems that the formation of straight helical rods does not favor peptide association into large channel structures. An explanation might be that the structural change in the molecule as a result of Pro-Ala replacement brings the glutamic acid residues at position 18 closer together. Thus electrostatic repulsive forces between negatively charged residues might be responsible for the reduced association number and the decreased stability of the Alam-A14 channels compared to the native peptide. Recently, lifetime differences have also been found to correlate with the interhelical hydrogen bonding capability (Molle et al., 1996). In Alam-A14 intramolecular hydrogen bonds are restored and the conformational change may disturb the suggested intermolecular glutamine 7 - ring stabilization in the alamethicin channels. Moreover, Pro-Ala substitution enhances the hydrophobicity of the peptide and might favor peptide-lipid contacts and reduce channel-stabilizing peptide-peptide interactions.

In summary, the conformational change causing a substantial increase in helix formation does not influence the packing of the helix bundles, but rather influences the uptake and release of monomers as well as the stability of the aggregates in the conducting states. The results suggest that bending at position 14 as a flexible element (Vogel et al., 1993) seems to be not so critical for the gating of voltage-dependent alamethicin ion channels. Such a conclusion is in accordance with the recent result of a structural investigation that provides evidence for a roughly linear conformation of alamethicin in the membrane-bound state (Barranger-Mathys and Cafiso, 1996).

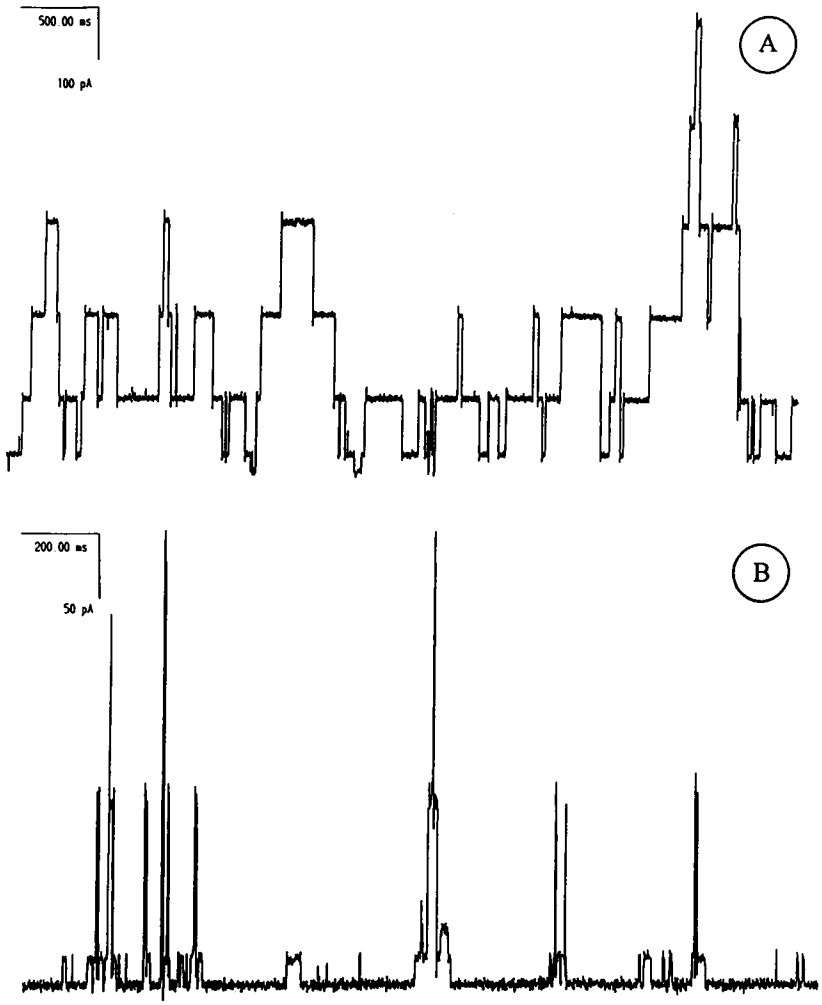

FIGURE 4 Representative single-channel traces induced by (*A*) 5×10^{-9} M Alam-P14 at 120 mV and (*B*) 30×10^{-9} M Alam-A14 at 130 mV. Electrolyte solution at both sides of a POPC/DOPE bilayer was 1 M KCl, room temperature.

An N- or C-terminal shift of proline causes a pronounced decrease in channel activity, as reflected by strongly reduced concentration and voltage dependencies. Interestingly, proline incorporated at positions 13, 15, and 16 changes the number but not the level of the detectable conductance states. The most significantly modulated parameter is channel kinetics. The channel life time is reduced, with the exception of the lowest conductance level found for Alam-P13 and Alam-P15, which exhibits high stability. Furthermore, the increased noise level of the open states argues for a destabilization of the bundle geometry of the channels of the alamethicin analogs.

The experimentally determined helicities of the alamethicin analogs with channel activity, Alam-P13, Alam-P14, Alam-P15, Alam-P16, are below 50% and exhibit serious differences. It is interesting to note that the sequences with proline following Aib (Alam-P14, Alam-P16) exhibit more than 40% helix in the lipid-bound state, whereas the peptides with Pro-Aib bonds (Alam-P13 and Alam-P15) display only ~25% helicity. The possible role of Aib-Pro- and Pro-Aib peptide bonds in the helicity of alamethicin is not yet understood and is the subject of further investigation. Nevertheless, the results confirm the conclusion that peptide helicity is of reduced importance for channel formation. Obviously, the main effect of the change in proline position next to position 14 is the disturbance of intermolecular peptide interactions, reflected by a reduced ability of the peptides to form large associates and changes in kinetics of

TABLE 4 Single-channel conductance levels (pS) of alamethicin analogs in POPC/DOPE membranes at room temperature

Peptide	1	2	3	4	5	6	7
Alam-P13	150	610	1360				
Alam-P14	**170**	**400**	**1300**	**2500**	**4000**	**5600**	**7200**
Alam-P15	140	440	1400	2770	4280		
Alam-P16	180	400	1010	2050			
Alam-A14	170	380	1200	2500			

TABLE 5 Mean-channel open lifetimes (in ms) of alamethicin analogs

Peptide	1	2	3	4	5	6	7
Alam-P13	118	18	13				
Alam-P14	**10**	**34**	**59**	**96**	**71**	**45**	**32**
Alam-P15	56	36	88	20	16		
Alam-P16	5	2	3	2			
Alam-A14	9	3	6	2			

uptake and release of peptide monomers. Interestingly, the activity reducing effect is more pronounced in analogs with proline shifted to the N-terminus compared to its introduction in the C-terminal side of the original position. Assuming that the N-terminal helical part of the peptide molecules is most important in stabilizing the peptide monomers in the channel arrangement (Vogel, 1987), modifications in this region may be expected to influence the channel properties dramatically. A disturbance of the main helix would also explain the loss of channel activity of Alam-P11 and Alam-P12. However, the helical potential of these two peptides was found to be comparably high (Table 2), suggesting that other factors also influence channel formation. Thus we have to consider the low affinity of these two peptides for neutral lipid bilayers. Taking into consideration that only a small number of bound peptides are arranged in channel structures (Archer et al., 1991), the probability of channel formation decreases with reduced binding. Furthermore, proline incorporation at position 11 or 12 might influence the interhelical hydrogen bonds between the glutamine residues at position 7 that are suggested to stabilize the channel structure (Molle et al., 1996). Furthermore, molecular dy-

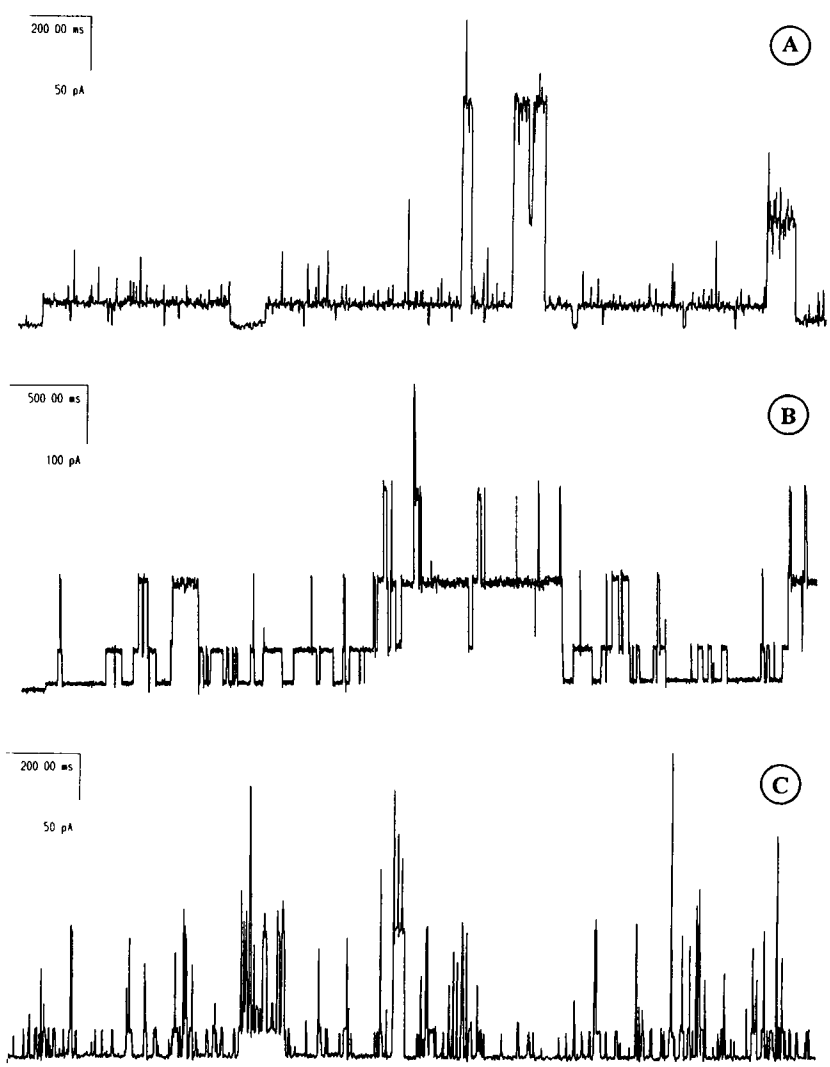

FIGURE 5 Representative single-channel traces induced by (*A*) 1×10^{-7} M Alam-P13 at 130 mV; (*B*) 0.5×10^{-7} M Alam-P15 at 120 mV; (*C*) 1×10^{-7} M Alam-P16 at 130 mV. The electrolyte solution at both sides of a POPC/DOPE bilayer was 1 M KCl, room temperature.

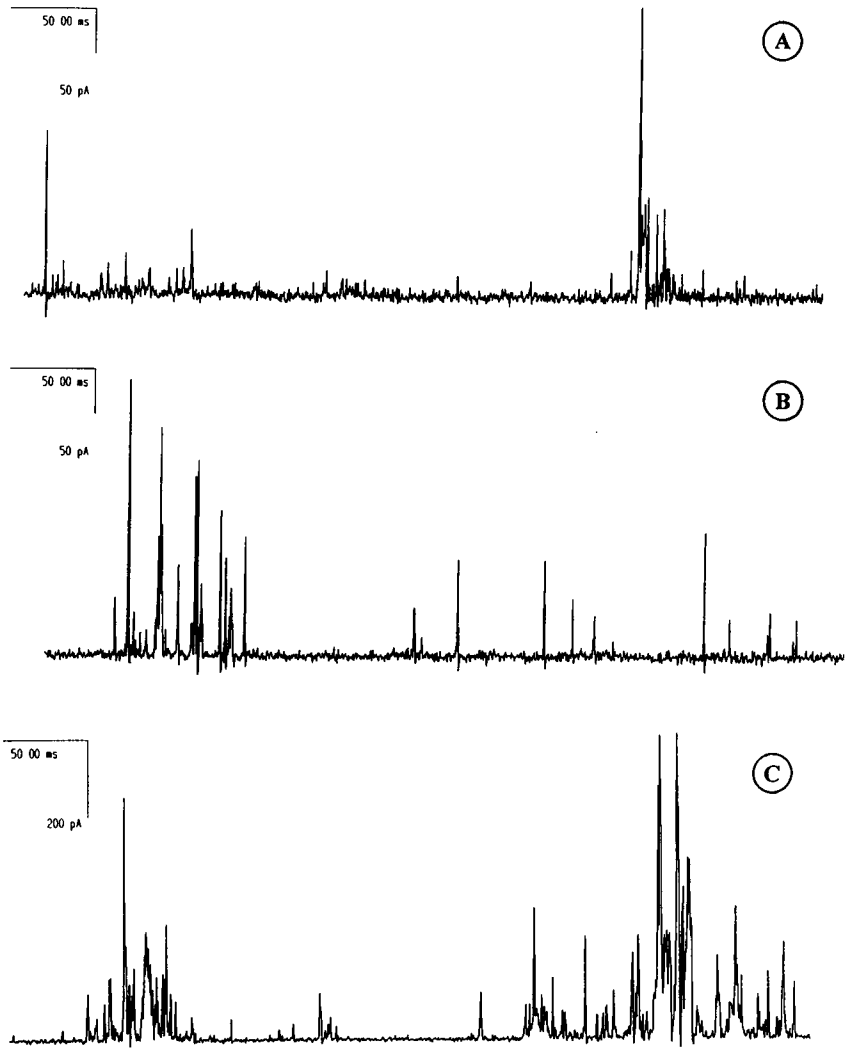

FIGURE 6 Representative single-channel traces induced by (*A*) 0.5×10^{-7} M Alam-P11 at 120 mV; (*B*) 4×10^{-7} M Alam-P12 at 150 mV; (*C*) 2×10^{-7} M Alam-P17 at 110 mV. The electrolyte solution at both sides of a POPC/DOPE bilayer was 1 M KCl, room temperature.

namic simulations reveal that Alam-P11 would result in a bending of the C-terminal helix into the presumed channel interior (i.e., toward the hydrophilic pore-lining residues), thus making association impossible, and Alam-P12 would adopt a structure with a kink of the helix toward the neighboring molecule in the channel arrangement, which is obviously also less favorable for channel stability (G. Krause, personal communication).

Proline at position 17 might cause a relatively high flexibility in the remaining C-terminal sequence, and intermolecular electrostatic repulsive forces between Glu^{18} residues should disturb associations, thus explaining the lack of channel activity of Alam-P17.

In conclusion, both Pro^{14} substitution by alanine and the change of the proline position do not prevent channel formation, but lead to a reduced number of conductance levels and a reduced probability of being open. With regard to concentration and voltage dependencies, average channel size, and channel lifetime, proline at position 14 in native alamethicin has reached its optimal position through the pressure of molecular evolution.

The authors thank Olivier Helluin for assisting with the electrophysiological experiments and Gerd Krause for his efforts in modeling the peptides.

REFERENCES

Archer, S. J., J. E. Ellena, and D. S. Cafiso. 1991. Dynamics and aggregation of the peptide ion channel alamethicin. *Biophys. J.* 60:389–398.

Barranger-Mathys, M., and D. S. Cafiso. 1996. Membran structure of voltage gated ion channel forming peptides by side-directed spin labeling. *Biochemistry.* 35:498–505.

Baumann, G., and P. Mueller. 1974. A molecular model of membrane excitability. *J. Supramol. Struct.* 2:538–557.

Boheim, G. 1974. Statistical analysis of alamethicin channels in black lipid membranes. *J. Membr. Biol.* 19:277–303.

Brachais, L., D. Davoust, and G. Molle. 1995a. Conformational study of a synthetic analogue of alamethicin. *Int. J. Pept. Protein Res.* 45:164–172.

Brachais, L., H. Duclohier, C. Mayer, D. Davoust, and G. Molle. 1995b. Influence of proline-14 substitution on the secondary structure in a synthetic analogue of alamethicin. *Biopolymers.* 36:547–558.

Cafiso, D. S. 1994. Alamethicin: a peptide model for voltage gating and protein-membrane interactions. *Annu. Rev. Biophys. Biomol. Struct.* 23:141–165.

Chandrasekhar, K., M. K. Das, A. Kumar, and P. Balaram. 1988. Molecular conformation of alamethicin in dimethylsulfoxide solution. *Int. J. Pept. Protein Res.* 32:167–174.

Chen, Y. H., J. T. Yang, and H. M. Martinez. 1972. Determination of the secondary structures of proteins by CD and optical rotary dispersion. *Biochemistry.* 11:4120–4131.

Duclohier, H., G. Molle, J.-Y. Dugast, and G. Spach. 1992. Proline are not essential residues in the "barrel-stave" model for ion channels induced by alamethicin analogues. *Biophys. J.* 63:868–873.

Esposito, G., J. A. Carver, J. Boyd, and I. D. Campell. 1987. High-resolution ^{1}H NMR study of the solution structure of alamethicin. *Biochemistry.* 26:1043–1050.

Fox, F. O., and F. M. Richards. 1982. A voltage gated ion channel model inferred from the cristal structure of alamethicin at 1.5 Å resolution. *Nature.* 300:325–330.

Franklin, J. C., J. F. Ellena, S. Jayasinghe, L. P. Kelsh, and D. S. Cafiso. 1994. Structure of micelle-associated alamethicin from ^{1}H NMR. Evidence for conformential heterogeneity in a voltage-gated peptide. *Biochemistry.* 33:4036–4045.

Fraternali, F. 1990. Restrained and unrestrained molecular dynamics simultation in the NVT ensemble of alamethicin. *Biopolymers.* 30: 1083–1099.

Gordon, L. G. M., and D. A. Haydon. 1972. The unit conductance channel of alamethicin. *Biochim. Biophys. Acta.* 255:1014–1018.

Gordon, L. G. M., and D. A. Haydon. 1975. Potential-dependent conductance in lipid membranes containing alamethicin. *Phil. Trans. R. Soc. London Ser. B.* 270:433–447.

Hall, J. E., I. Vodyanow, T. M. Balasubramanian, and G. R. Marshall. 1984. Alamethicin: a rich model for channel behaviour. *Biophys. J.* 45:233–247.

Hanke, W., and G. Boheim. 1980. The lowest conductance state of the alamethicin pore. *Biochim. Biophys. Acta.* 596:456–462.

Kaduk, C., H. Wenschuh, M. Beyermann, K. Forner, L. A. Carpino, and M. Bienert. 1995. Synthesis of Fmoc-amino acid fluorides via DAST, an alternative fluorinating agent. *Lett. Pept. Sci.* 2:285–288.

Kelsh, J. P., J. F. Ellena, and D. S. Cafiso. 1992. Determination of the molecular dynamics of alamethicin using 13C NMR: implications for the mechanism of gating of a voltage-dependent channel. *Biochemistry.* 31:5136–5144.

Meyer, P., and F. Reusser. 1967. A polypeptide antibacterial agent isolated from *Trichoderma viride. Experientia.* 23:85–86.

Molle, G., J.-Y. Dugast, G. Spach, and H. Duclohier. 1996. Ion channel stabilization of synthetic alamethicin analogs by rings of inter-helix H-bounds. *Biophys. J.* 70:1669–1675.

Montal, M., and P. Mueller. 1972. Formation of bimolecular membranes from monolayers and study of their properties. *Proc. Natl. Acad. Sci. USA.* 69:3561–3566.

North, Ch. L., J. C. Frankline, R. G. Bryant, and D. S. Cafiso. 1994. Molecular flexibility demonstrated by paramagnetic enhancement of nuclear relaxation. Application to alamethicin. *Biophys. J.* 67: 1861–1866.

Sansom, M. S. P. 1991. The biophysics of peptide models of ion channels. *Prog. Biophys. Mol. Biol.* 55:139–235.

Sansom, M. S. P. 1993. Structure and function of channel forming peptaibols. *Q. Rev. Biophys.* 26:365–421.

Vanhoof, G., F. Goossens, I. de Meester, D. Hendriks, and S. Scharpe. 1995. Proline motifs in peptides and their biological processing. *FASEB J.* 9:736–744.

Vogel, H. 1987. Comparison of the conformation and orientation of alamethicin and mellitin in lipid membranes. *Biochemistry.* 26:4562–4572.

Vogel, H., L. Nilsson, R. Riegler, S. Meder, G. Boheim, W. Beck, H.-H. Kurth, and G. Jung. 1993. Structural fluctuations between two conformational states of a transmembrane helical peptide related to its channel-forming properties in planar lipid membranes. *Eur. J. Biochem.* 212: 305–313.

Wenschuh, H., M. Beyermann, S. Rothemund, L. A. Carpino, and M. Bienert. 1995. Multiple solid phase synthesis via Fmoc-amino acid fluorides. *Tetrahedron Lett.* 36:1247–1250.

Woolfson, D. N., R. J. Mortishire-Smith, and D. H. Williams. 1991. Conserved positioning of proline residue in membrane-spanning helices of ion channel proteins. *Biochem. Biophys. Res. Commun.* 175:733–737.

Woolley, G. A., and B. A. Wallace. 1992. Model ion channels: gramicidin and alamethicin. *J. Membr. Biol.* 129:109–136.

Yee, A. A., R. Babiuk, and J. D. J. O'Neil. 1995. The conformation of an alamethicin in methanol by multinuclear NMR specroscopy and distance geometry/stimulated annealing. *Biopolymers.* 36:781–792.

Yee, A. A., and J. D. J. O'Neil. 1992. Uniform ^{15}N labeling of a fungal peptide: the structure and dynamics of an alamethicin by ^{15}N and ^{1}H NMR spectroscopy. *Biochemistry.* 31:3135–3143.